Supplementary Material for

Mutation in Transforming Growth Factor Beta Induced protein associated with Granular Corneal Dystrophy Type 1 Reduces the Proteolytic Susceptibility through Local Structural Stabilization

Jarl Underhaug*#[1], Heidi Koldsø†[2], Kasper Runager‡, Jakob Toudahl Nielsen*, Charlotte S. Sørensen‡, Torsten Kristensen‡, Daniel E. Otzen‡, Henrik Karring‡[3], Anders Malmendal*[4], Birgit Schiøtt†, Jan J. Enghild‡[5], and Niels Chr. Nielsen*[5]

*Center for Insoluble Protein Structures (inSPIN), Interdisciplinary Nanoscience Center (iNANO) and Department of Chemistry, Aarhus University, Gustav Wieds Vej 14, DK-8000 Aarhus C, Denmark;

#Department of Bimedicine, University of Bergen, Jonas Lies vei 91, NO-5009 Bergen, Norway

†Center for Insoluble Protein Structures (inSPIN), Interdisciplinary Nanoscience Center (iNANO) and Department of Chemistry, Aarhus University, Langelandsgade 140, DK-8000 Aarhus C, Denmark; and ‡Center for Insoluble Protein Structures (inSPIN), Interdisciplinary Nanoscience Center (iNANO) and Department of Molecular Biology and Genetics, Aarhus University, Gustav Wieds Vej 10, DK-8000 Aarhus C, Denmark

[1]Present address: Department of Biomedicine, University of Bergen, Norway
[2]Present address: Department of Biochemistry, University of Oxford, Oxford OX1 3QU, United Kingdom
[3]Present address: Department of Chemical Engineering, Biotechnology and Environmental Technology, Faculty of Engineering, University of Southern Denmark, DK-5230 Odense M, Denmark.
[4]Present address: Department of Biomedical Sciences, Faculty of Health Sciences, University of Copenhagen, DK-2200 Copenhagen N, Denmark.

[5]To whom correspondence should be addressed: Niels Chr. Nielsen, Center for Insoluble Protein Structures (inSPIN), Interdisciplinary Nanoscience Center (iNANO) and Department of Chemistry, Aarhus University, Gustav Wieds Vej 14, DK-8000 Aarhus C, Denmark. E-mail: ncn@inano.au.dk and Jan J. Enghild, Center for Insoluble Protein Structures (inSPIN), Interdisciplinary Nanoscience Center (iNANO) and Department of Molecular Biology and Genetics, Aarhus University, Gustav Wieds Vej 10, DK-8000 Aarhus C, Denmark, jje@mb.au.dk,

Supplementary Experimental Procedures

Construction of cDNA

The human FAS1-4 cDNA clone encoding residues 502-634 (for the WT FAS1-4 domain construct) or 502-634 (for the Arg555Trp FAS1-4 domain construct) in TGFBIp was obtained from a human placenta cDNA library cloned in the pCMV-SPORT6 vector. An additional full-length WT FAS1-4 domain, residues 502-657, was also made. For all constructs, an Ala-Gly dipeptide was included at the N-terminus to facilitate cleavage by the SUMO protease as described below. The gene encoding the Arg555Trp mutant of human TGFBIp was constructed by introducing point mutation in a QuikChange reaction (Stratagene) using the cloned WT *TGFBI* gene as template. Arg555Trp contained an additional spontaneous mutation, Pro634Ala, which was not present when sequencing the clone. The mutation has been selected during colony plating and single colony picking after transformation into *E. coli* strain BL(21)DE3. The mutation was discovered on NMR analysis and was ignored as it did not affect the protein structure significantly. The Champion pET SUMO Protein Expression System (Invitrogen) was used for expression of the protein. The pET SUMO vectors were transformed into competent One Shot® Mach1-T1 competent *E. coli* cells and the plasmids were isolated. The plasmids were then

transformed into One Shot® BL21(DE3) *E. coli* cells. The suspension of cells was then spread onto the surface of a Lysogeny broth (LB) agar plate containing the antibiotic kanamycin. The plate was incubated overnight at 37 °C.

Chemical Shift Analysis

Two types of analyses of the chemical shifts were performed. One was performed to validate the correctness of the derived structures and MD ensembles, while the other was used to correlate changes in structure to changes in chemical shifts. To validate the structures, and observed, $\delta^{obs}(i)$, and predicted, $\delta^{pred}(i)$, chemical shifts were compared and the pseudo energy is defined as a sum of scaled squared differences between the observed and predicted chemical shifts scaling with the typical standard deviation from a database of structures $E_{shift} = \frac{1}{N}\sum_i^N \left(\left(\delta^{obs}(i) - \delta^{pred}(i)\right)/\sigma(i)\right)^2$. In this expression each predicted chemical shift, $\delta^{pred}(i)$, is the average of all predicted values for that particular atom for each member of NMR ensemble or snapshots from the MD trajectory. For the MD trajectories, the average pseudo energy was used and the standard deviation was calculated from three independent trajectories. No standard deviation was estimated for NMR ensemble.

First, ρ_{obs} reports a residue-based weighted sum of differences between the chemical shift for the WT, δ_{wt}^{obs}, and the chemical shift for the Arg555Trp mutant, δ_W^{obs}, defined as: $\rho_{obs} = \sqrt{\frac{1}{N}\sum_i^N \left(\left(\delta_{wt}^{obs}(i) - \delta_W^{obs}(i)\right)/\sigma(i)\right)^2}$. To separate the primary effect of substituting Arg555 to Trp555 from the effect of possible rearrangements caused by the mutation, we engineered a structure by replacing Trp555 in the mutant structure back to Arg555. Since, naturally, no experimental data is available for this engineered structure, the corresponding chemical shifts (δ_R) were predicted for this structure. The δ_R chemical shifts were compared to the chemical shift predicted based on the WT and mutant structures. An RMSD chemical shift value ρ_W was derived to quantify the predicted effect caused exclusively by the Trp555 residue compared to the Arg555 residue in the FAS1-4 domain structure: $\rho_W = \sqrt{\frac{1}{N}\sum_i^N \left(\left(\delta_R^{pred}(i) - \delta_W^{pred}(i)\right)/\sigma(i)\right)^2}$. In the two formulas above, the scaling parameter $\sigma\,(i)$ is the average standard deviation among the chemical shifts for a fixed amino acid and secondary structure type taken from the BMRB website. Another RMSD, ρ_{struct}, was calculated describing the predicted effect of rearrangement in the tertiary structure caused by the mutation, i.e., $\rho_{struct} = \sqrt{\frac{1}{N}\sum_i^N \left(\left(\delta_R^{pred}(i) - \delta_{wt}^{pred}(i)\right)/s_{tot}(i)\right)^2}$ using $s_{tot}(i) = \sqrt{s_R^2(i) + s_{wt}^2(i)}$ taken as the sample standard deviation among the 10 conformers in the structural ensemble (we note the different scaling compared to the first two equations).

Supplementary Figures

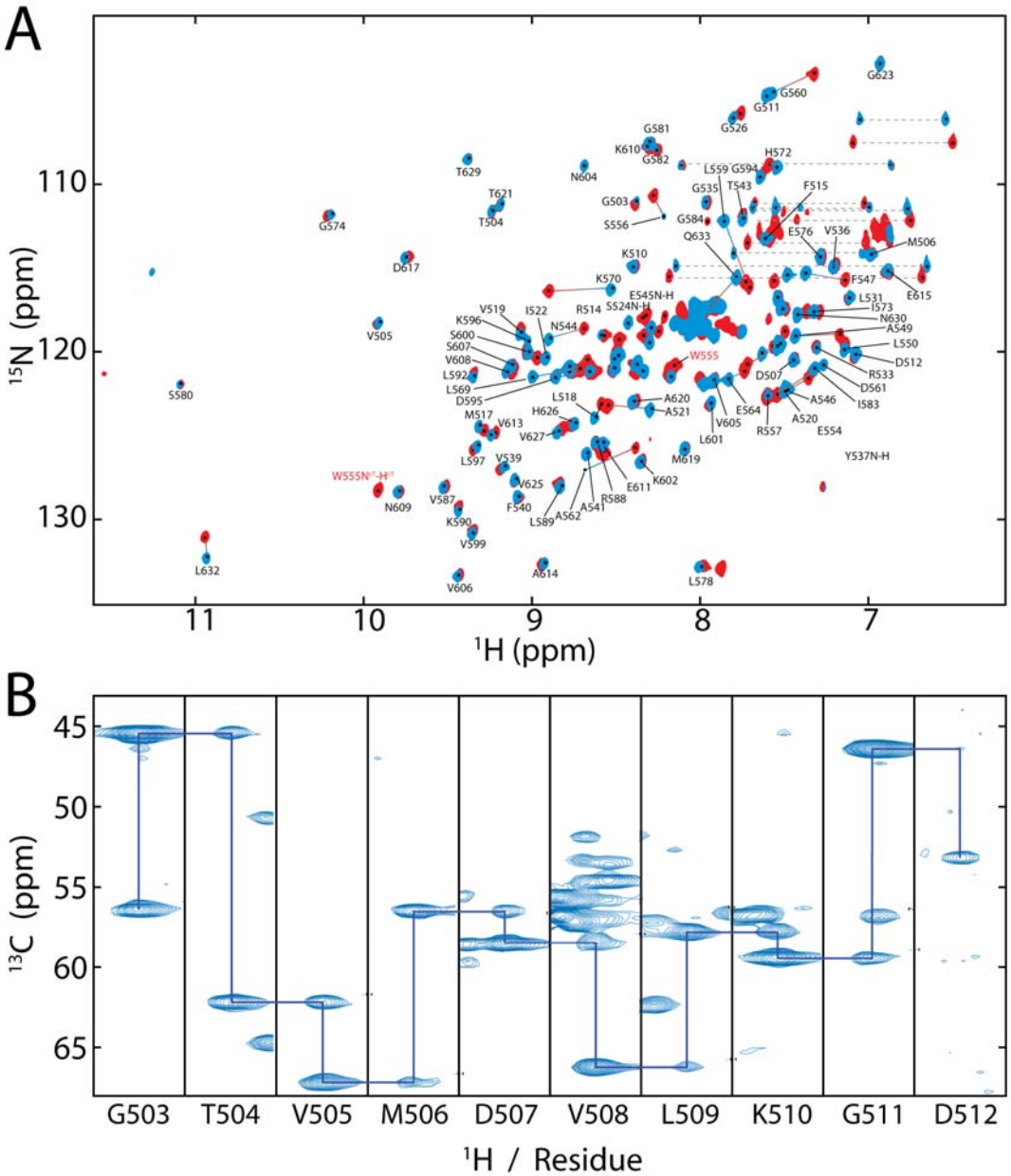

Figure S1. NMR spectra of the FAS1-4 domains. (A) The ^{1}H-^{15}N HSQC spectrum of the WT FAS1-4 domain (blue) overlaid on the spectrum of the Arg555Trp mutant domain (red). The spectra are very similar, i.e., most of the Arg555Trp mutant domain signals are perfectly hidden by the WT domain signals. Only a small portion of the signals is significantly shifted. This indicates that the structures are almost identical. Assignments of the backbone of WT has been added where space permits. Some regions are too crowded for individual peaks to be discerned. The coloured lines indicate movement of the peaks induced by the mutation, and dashed lines indicate are used to highlight some side-chain peaks. (B) A selection of strips from a HNCA spectrum of the WT FAS1-4 domain structure.

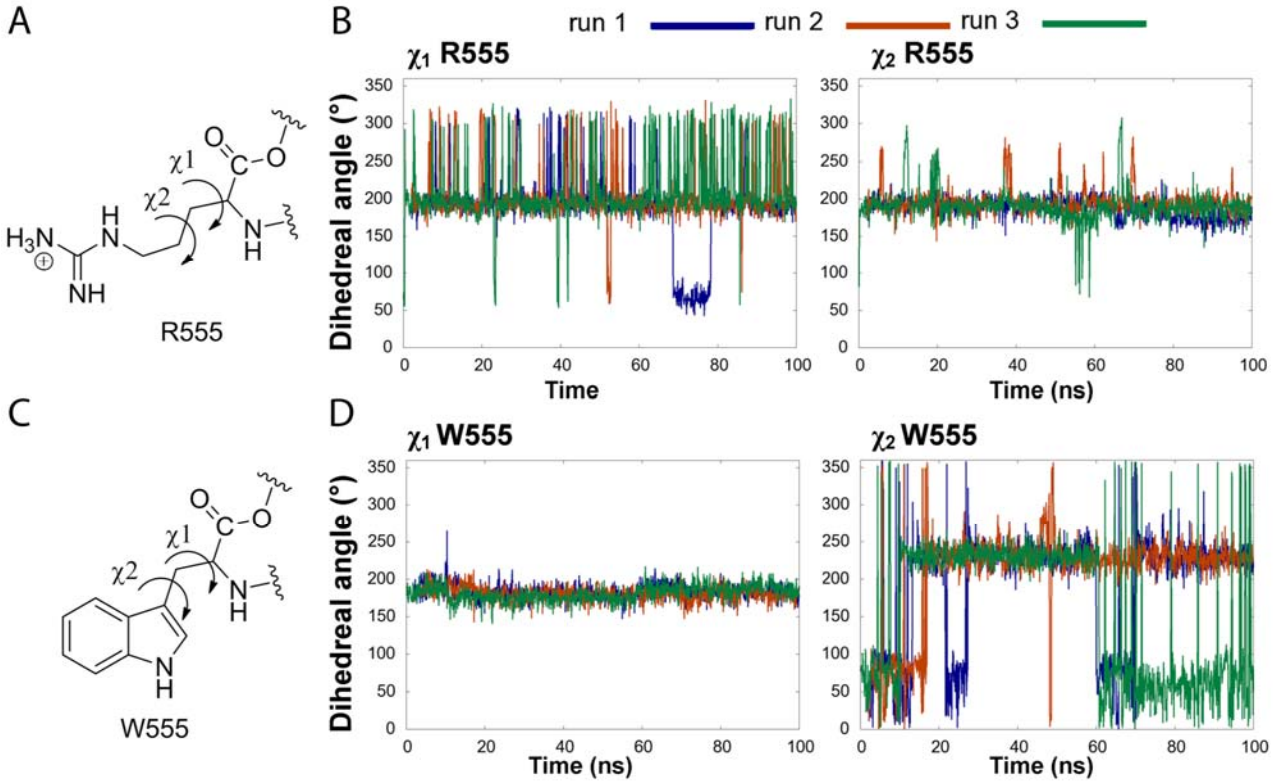

Figure S2. MD simulations of residue 555 side-chain motion in the WT and Arg555Trp FAS1-4 domains. Side chain rotations of Arg555 in the WT FAS1-4 domain and Trp555 of the Arg555Trp mutant structure are illustrated by the χ_1 and χ_2 rotational angles. (A) The χ_1 and χ_2 dihedral in the arginine side chain. (B) The χ_1 of Arg555 fluctuates between the *anti* and the *gauche* conformation continuously throughout the simulation, whereas the χ_2 dihedral of Arg555 in the WT system remains stable in the *anti* conformation during the simulation. (C) The χ_1 and χ_2 dihedral in the tryptophan side chain of the Arg555Trp mutant structure. (D) In the Arg555Trp mutant domain the χ_1 angle of Trp555 stays in the *anti* conformation throughout the simulation. The χ_2 angle on the contrary fluctuates between the initial *gauche* conformation and the *anti* conformation. This indicates a flip of the aromatic moiety during simulation. Only in run 3 the χ_2 angle jumps back into the *gauche* conformation during the 100 ns trajectory.

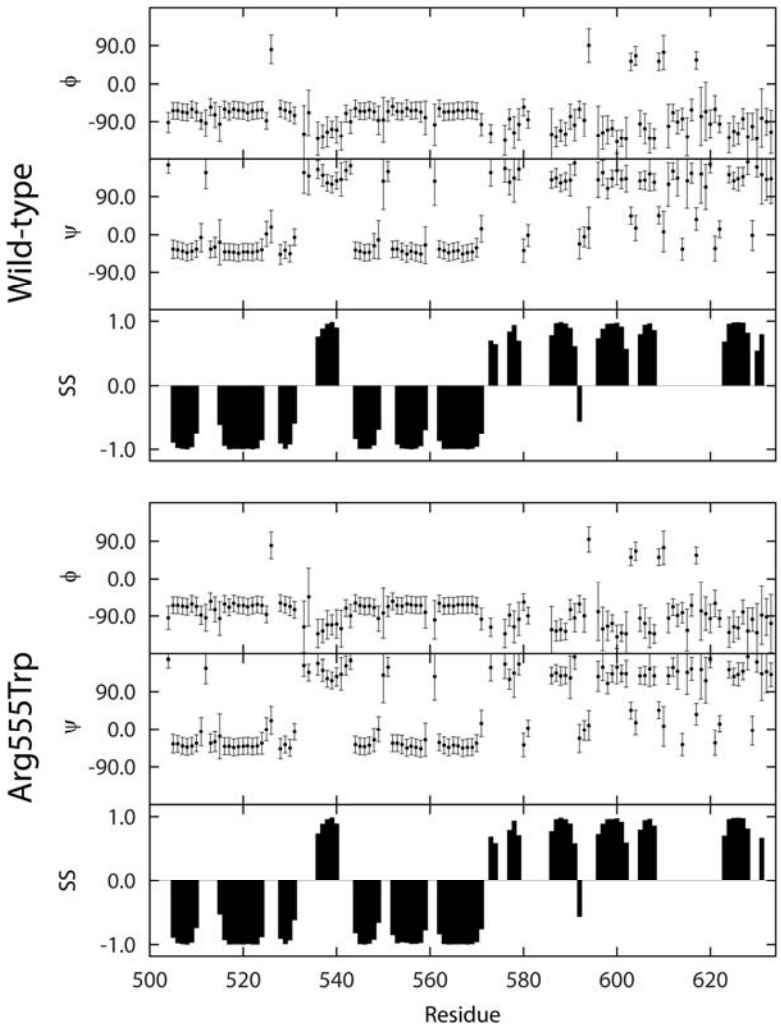

Figure S3. Dihedral angle constraints used when calculating the NMR structures. The three upper panels show the ϕ and ψ dihedral angle constraints from TALOS+ which were used in the structure calculation, as well as the predicted secondary structures (SS) for the wild-type protein. For the predicted secondary structure -1 indicate α-helix, while +1 indicate β-sheet. The three lower panels show the corresponding values for the Arg555Trp mutant.